

AN EXPERIMENTAL AND NUMERICAL INVESTIGATION INTO FLOW PHENOMENA LEADING TO WASTEWATER CENTRIFUGAL PUMP BLOCKAGE

Connolly R.*¹, Breen B¹. and Delauré Y².

¹Sulzer Pump Solutions Ireland Ltd.,
Wexford, Ireland.

²School of Mechanical and Manufacturing Engineering,
Dublin City University, Ireland.
E-mail: robert.connolly@sulzer.com

ABSTRACT

The work covered in this paper had the objective of investigating key factors in single vane pump impeller blockage using both CFD and experimental analysis. Single vane centrifugal pumps can be found in wastewater applications, where suspended solids, fibers and other flexible material can build up on the pump impeller and cause blockage and failure. It is in the pump manufacturer's interest to design blockage resistant components while still maintaining hydraulic efficiency. Testing was conducted on a large variety of centrifugal wastewater pumps at different operating points in a purpose built test rig with suitable test material. A pump which had varying blockage performance depending on operating point was chosen for further study with CFD. Transient simulations with the SA-DDES turbulence model were carried out with the same operating conditions as in the experimental analysis. CFD has been used to highlight flow features likely to lead to such blockage, while experiments provided some insight into the significance of certain key parameters. An analysis of the CFD results showed a significant correlation between pump blockage performance and radial velocity components within the fluid domain, specifically in the impeller region. Sensitivity to blockage was found to vary with the head required of the pump. This sensitivity was further explained when applying the hypothesis of the impact of velocity components on the likelihood of pump blockage.

INTRODUCTION

In recent decades there has been significant improvement in access to water sanitation [1]. With increasing global populations, the demand has never been higher for reliability in wastewater systems. Wastewater pumps are integral components of wastewater systems, featuring in collection transportation and treatment processes and as a major contributor to system failures, they are a key concern for reliability [2]. A common cause of waste-water pump failure is related to soft blockage, where fibrous material catches on the impeller and builds up, leading to high motor current and thermal overload. Single vane impellers in both open and closed configurations allow for larger channel size and easier passage of larger solids. Framework agreements such as [3] insist on a minimum solids passage size for installations in their jurisdiction. Many waste-water pump manufacturers offer a single vane impeller in order to meet requirements regarding minimum solids passage and blockage performance.

NOMENCLATURE

Q	Volumetric flow rate
BI	Blockage index
z_{LA}	Impeller blade number
RI	Rag incidence
A	Cross sectional area
l	length
ω	Rotational speed
H	Head
p	Pressure
ρ	Density
g	Acceleration due to gravity
z	Elevation
v	Velocity
y^+	non dimensional cell wall distance

Subscripts & Superscripts

rad	radial
tan	tangential
LE	Leading edge
rot	rotational

An example of a single vane pump hydraulic can be seen in Figure 1. Significant experimental research relating to impeller blockage has been carried out during hydraulic development of new products at Sulzer Pumps. While CFD has been commonly used in the design stage for hydraulic performance, recently experimental research has been increasingly supplemented by CFD in order to further understand how flow features affect impeller blockage.

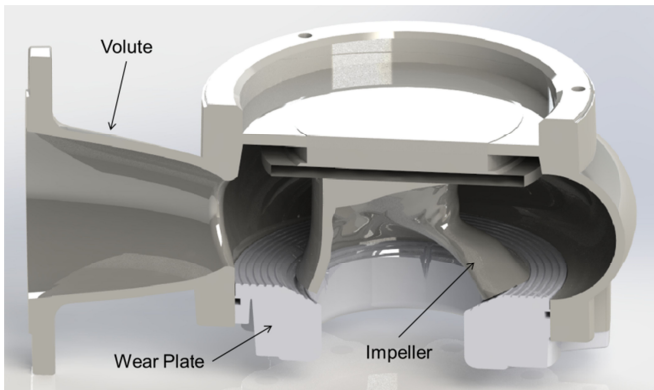


Figure 1. Typical single vane waste-water pump hydraulic components.

EXPERIMENTAL

An acceptable and realistic test method was needed in order to test a wide range of pumps with material that accurately reflects the conditions experienced by pumps in the field.

The test method used in this study was based on that of McEvoy, [4]. Tests were repeated over three different flow rates covering typical operating range of wastewater pumps. The volumetric flow rate at the Best Efficiency Point, Q_{bep} was used, as well as at flow rates 30% above and below this value, $Q_{bep+30\%}$ and $Q_{bep-30\%}$ respectively. Three independent tests were repeated at each flow rate with each test run involving the introduction of 10 blockage samples. A score was assigned for each flow rate, based on the percentage of samples passed by the pump. The average of these three flow rates gave the pump blockage index (BI). The BI is defined as the ratio of samples passed, B_p to the total number of samples introduced, B_i , $BI = \frac{B_p}{B_i} \times 100$.

Pumps tested were of standard type used in municipal wastewater application, as would be seen in the field.

In order to supplement and further inform the research, a high speed camera was used to record the hydraulic both passing the rag and blocking. The camera, which was capable of recording at 1000fps, provides some insight into how the test material interacts with the fluid and the pump impeller surface in addition to the forces which act upon it.

In order to reliably carry out a test that is representative of field conditions, it was necessary to select a suitable test material. An analysis of blockages was carried out on three sites and samples taken for classification. Most blockages contained cloth of non-woven synthetic fibres, typically the outer casing of sanitary towels and disposable domestic wipes. A study of waste-water constituents has found results consistent with samples taken locally [5].

A test rig was designed and built in order to test a large range of pumps, 1.3kW to 90kW. The test hardware on the tank included flow-meters and pressure transducers on both inlet and outlet pipes (or did you mean something else) in order to accurately establish the duty point at which the pumps were being tested. A pinch valve was located between the pressure

tapping and the flow-meter to maintain the desired flow rate. Perspex windows were located directly below the coupling point of the test pump and at the tank sides. This permitted visual inspection and recording of rag behaviour as it interacts with the pump suction stream and impeller. The high speed camera in the blockage test rig was used to compare blockage behaviour of each of the shortlisted sample materials at high flow, low flow and best efficiency point.

EXPERIMENTAL RESULTS

McEvoy [4], states that leading edge blockage is the most prominent type of blockage found in this type of centrifugal pump in wastewater application. It was decided to focus this research on the contributing factors to leading edge blockage. A large number of observations were made of pump blockage with the high speed camera equipment at the specified test flow rates. When passing through the pump, the rag was observed to come through the inlet, along the impeller suction surface, past the impeller trailing edge, around the leading edge and out of the volute via the discharge after one or two rotations. A typical process of leading edge blockage was the rag being caught either side of the impeller leading edge as a result of not being moved outwards quickly enough. The action of consistent leading edge blockage was observed and recreated in 3D CAD. Figure 2 shows how the rag is seen to enter the pump towards the suction surface via the inlet. With the flow split between the suction and pressure surfaces, it was noted that rag orientation on entering the pump can have an impact on blockage, as per Figure 2. [i]. If the rag is found to be simultaneously distributed across the streamlines towards both the pressure and suction surfaces then it is likely to block, [ii]. As the rag approaches the impeller surface, it is already being streamed along both pressure and suction surface by the fluid flow, which is slower than the impeller rotational speed, [iii]. If pressure forces pinning the rag on either side of the impeller leading edge are in equilibrium, it is likely to remain stuck in this position [iv].

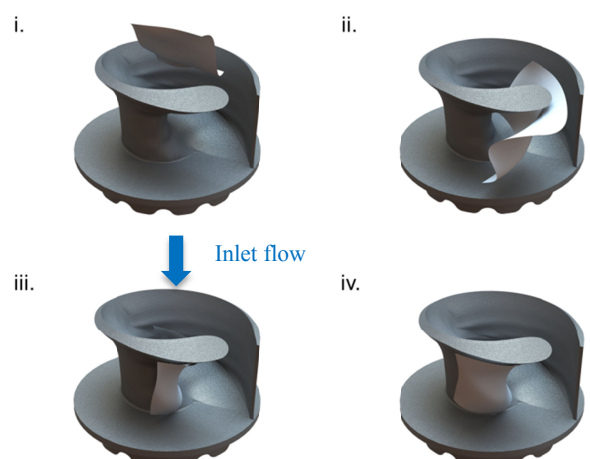


Figure 2: Stages of rag blockage based on experimental observation

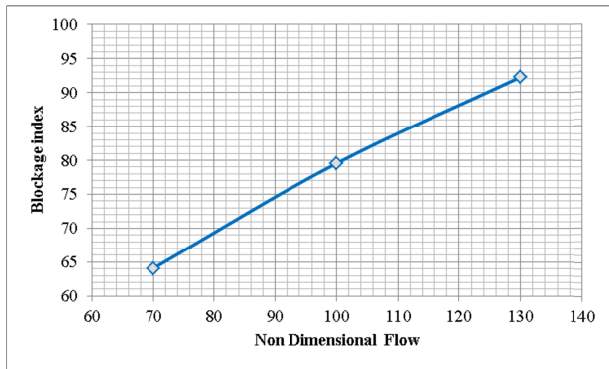


Figure 2 Averaged blockage performance at multiple non-dimensionalised flow rates

Average results indicated that a correlation between relative flow rate and Blockage Index does exist (see Figure 3). This can be explained by a number of key factors shown to influence the blockage. The anti-clogging performance should increase in proportion to:

- The volumetric flow rate Q or the average radial flow velocity over the impeller opening between its leading and trailing edge v_{rad} . High flow rate through the pump strongly influences the speed of ejection of the rag out of the impeller region into the pump volute.
- The tangential flow velocity of the impeller opening v_{tan} . If the flow transporting the rag as it is ejected into the volute past the trailing edge is at a higher tangential velocity than the speed of the leading edge, it is less likely to be caught up by the impeller before it is fully transported into the rotating flow of the volute region. This however is difficult to quantify from purely geometric consideration.

The opposite effect should occur by increasing:

- The area of the gap A between the impeller leading and trailing edge: the smaller this area the stronger the flow ejection velocity which helps to clear the rag off the impeller. The number of blades z_{LA} may also have an effect as an increase in z_{LA} is likely to lead to a smaller gap. z_{LA} however, also impacts on the general hydrodynamic performance, but the effect in this case is difficult to qualify.
- The length of the rag, l : as the rag flows out of the interior part of the impeller, past the trailing edge into the volute it finds itself in a flow which may be circulating around the volute at lower speed than the leading edge of the impeller. If this is the case the impeller can catch up with the rag, eventually leading to a rag wrapping itself around the impeller. This is more likely to occur for a longer rag in particular if its trailing end is kept back by interaction with the inlet

wall or the wear plate. It may be pinned against the wall by pressure or exposed to shear stresses due to friction against the wall surface.

- The rotational speed of the impeller ω : the faster the impeller for a fixed inlet flow rate, the more likely it is to catch the rag. An increase in the rotational speed of the impeller can also alter the hydrodynamic performance affecting the ratio of radial to tangential velocity at the exit from the impeller which is key to the anti-clogging performance. This however is difficult to quantify without taking into account the volute and impeller geometries and details of their effects on the flow. This would suggest that a purely statistical analysis focussing on the rotational speed may fail to show strong correlation.

To summarize it can be expected that the likelihood of clogging should increase in proportion to A , l and possibly ω and inversely to Q . A non-dimensional rag index can then be defined as follows:

$$RI = \frac{A\omega}{Q} = \frac{dhl\omega}{Q}$$

An average of the experimental results of three different pump families tested in this study at three different flow rates do confirm that an inverse correlation between rag incidence and blockage index [Figure 4] exist.

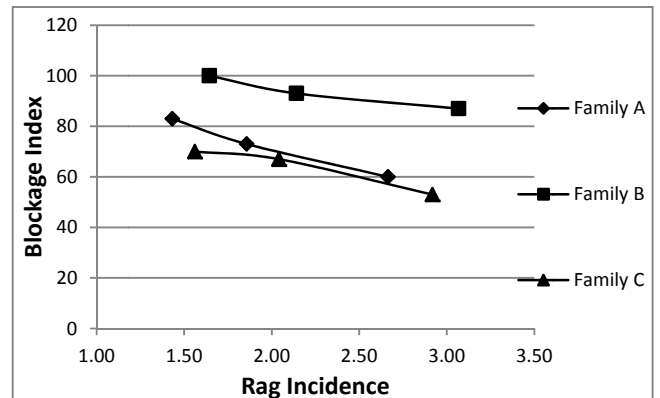


Figure 3 Rag Incidence vs. Blockage Index for 3 different pump families

Although ensemble averages suggest a non-negligible dependence of the Blockage Index on Rag Incidence, it must also be recognised that there is significant scatter in the data (see Figure 4-5). Blockage Index does not account for more complex interactions of rag and wear plate or variance in rag orientation at pump entry.

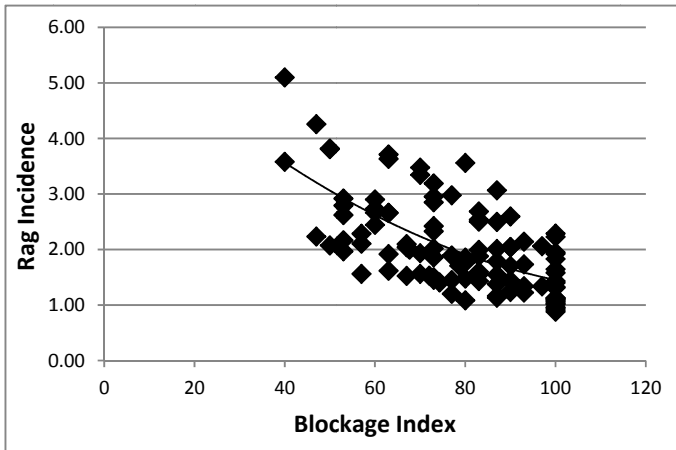


Figure 4 Blockage Index vs. Rag Incidence for full data set at each test flow rate

It can be hypothesised from the above results that as the rag moves through the pump driven by the through flow of the fluid, it can be intercepted by the impeller leading edge before it can be carried to a radial position outside of the leading edge. Once it has become trapped on the leading edge the rag is not be moved easily as forces driven by both the fluid inertia and impeller rotation ensure adhesion to the impeller.

NUMERICAL METHOD

A numerical approach was adopted to help confirm experimental results and interpretations. The pumps and other rotating equipment by CFD presents several specific challenges. The type of pump considered in this study exhibits flows which are highly time dependent so that simpler quasi-steady models are generally not suitable. Kaupert [6] reported in 1999 on the highly transient pressure field within a 7 blade centrifugal pump, while DeSouza [7] demonstrated computational results which had pump periodic pressure fluctuation by as much as 30%. In the case pump blockage study it is important that the transient processes characterising the interaction with the moving impeller are correctly captured. This means having to rely on a sliding mesh model. A Spalart-Allmaras Detached Eddy Simulation turbulence model was also used in this study in order to better resolve turbulent vortices.

A hexahedral mesh which contained $\sim 65 \times 10^5$ cells with a wall adjacent mesh characterised by y_{mean}^+ of 116, y_{min}^+ of 6 and y_{max}^+ of 300 on the impeller [8]. A review of literature has found that a similar y^+ resulted in accurate prediction of pressure coefficient predictions with an identical turbulence model [9]. The mesh contains 4mm cells in open areas with proximity refinement at the impeller in four steps where cells are split 8 times. 4 prism layers with a growth rate of 1.2 are used in the inflation layer. The pump was simulated for a minimum of 6 impeller revolutions and the average pressure and velocity values over the last rotation were used to calculate pump head with Eq.8.

$$Hp = \frac{p_2 - p_1}{\rho g} + z_2 - z_1 + \frac{v_2^2 - v_1^2}{2g} \quad (1)$$

The results for computational head were then compared with head and flow from the experimental pump curve. The results of this can be seen in Figure 5, where head and flow have been normalised to best efficiency point where $Q^* = \frac{Q}{Q_{BEP}}$.

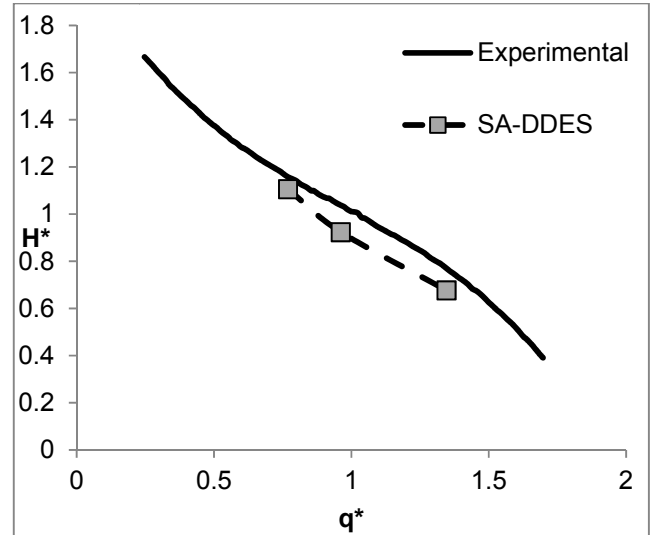


Figure 5 Computational Validation against Experimental Results

The comparison of the computational curve versus the experimental curve shows that the predicted pump head from CFD at $Q_{BEP}-30\%$, Q_{BEP} , and $Q_{BEP}+30\%$ is 4%, 11% and 13% respectively. Generally an acceptable level for quantitative analysis is $\leq 10\%$. Direct comparison is not as important in this case as a qualitative analysis is being carried out rather than a quantitative study.

NUMERICAL RESULTS AND DISCUSSION

Results were post processed in ANSYS CFD post. In addition to the inlet pressure plane a number of other analysis planes were inserted in the domain to study the fluid around the blade and volute at each flow rate [Figure 6].

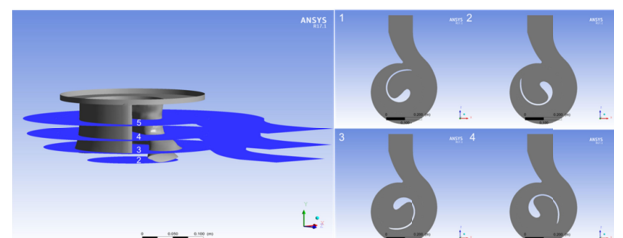


Figure 6 Left, Projection view of Impeller and 4 Analysis Planes. Right, Cross Section of Flow Domain at 4 Impeller Positions

Observations made during the experimental part of this work found that leading edge blockage was most prevalent at the coincident locations of the area where analysis Planes 4 and

5 can be seen in Figure 6. Plane 2 was chosen in order to analyse the flow at the pump inlet, while plane 3 was chosen to examine why no blockage was seen over this area of the pump.

The CFD results were analysed in terms of the components of flow in the radial and tangential directions with respect to the axis of rotation of the impeller:

$$v_{tan} = -\frac{r_z}{\sqrt{r_x^2 + r_z^2}}V_x + V_z \frac{r_x}{\sqrt{r_x^2 + r_z^2}} \quad (2)$$

$$v_{rad} = \frac{r_x}{\sqrt{r_x^2 + r_z^2}}V_x + V_z \frac{r_z}{\sqrt{r_x^2 + r_z^2}} \quad (3)$$

This made it possible to compare the speed of rotation of the flow v_{tan} with the circumferential velocity of the impeller leading edge $v_{l.e.}$ while taking account of the radial flow. It can be assumed that $v_{tan} > v_{l.e.}$ would increase the risk of blockage as the impeller can catch up with the rag. A higher velocity in the radial direction v_{rad} however should have the opposite effect by helping to flush the rag from the inner part of the impeller.

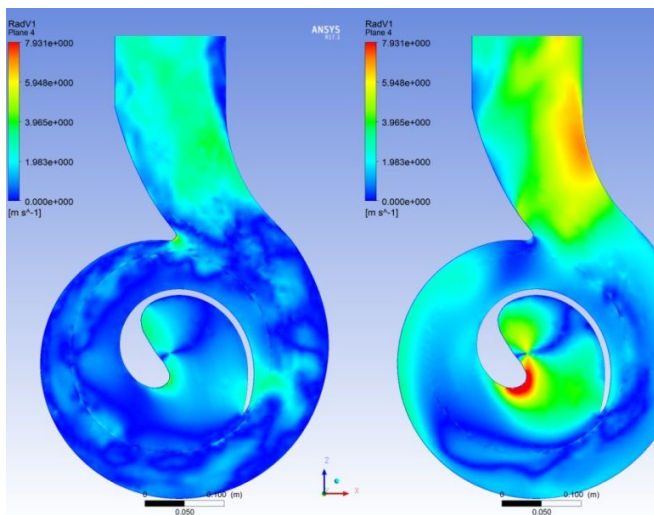


Figure 7 v_{rad} on Plane 4 at $Q^*=0.68$ (left) and $Q^*=1.11$ (right)

An analysis v_{rad} and v_{tan} on the selected planes does provide some useful information. Comparing flow predicted at high and low pump flow rates over Plane 4 where blockage does occur (Figure 7,8), there appears to be a relationship between the ratio of radial to tangential planar velocity and the probability of blockage occurring. This is based on an analysis of the flow between the leading and trailing edge of the impeller. **Figure 7** shows a much higher value of radial velocity at high flow rate compared to low flow rate. An area of high radial velocity can clearly be seen at the impeller leading edge where the relative flow incident angle β_{1-en} is higher, as described by Paresh [10]. This essentially means that as the flow rate changes the fluid incidence angle relative to the impeller leading edge also changes. Conversely, as Q^*

increases, tangential velocity decreases, [Figure 6-5]. This is in line with [11] and also the experimental results. One hypothesis for an inverse relationship between Q^* and v_{tan} is that there is less through-flow at low flow rates but very similar impeller rotational speed, causing a higher level of recirculation. As the fluid will remain for a longer time in the domain at low flow, there is a longer time for the impeller to impart energy on to the fluid. Also as separation on the pressure surface is less likely to happen at low flow rates [12], the fluid may be more likely to stay attached to the blade allowing more transfer of angular momentum. The higher levels of recirculating flow can only serve to increase the probability of blockage due to the fact that the impeller is exposed to the rag for a longer time while rotating with the impeller. This is particularly true if the trailing part of a longer rag is still within the leading edge region of the impeller, slowing its ejection into the outer part of the volute. The impeller leading edge is then more likely to catch up with the rag.

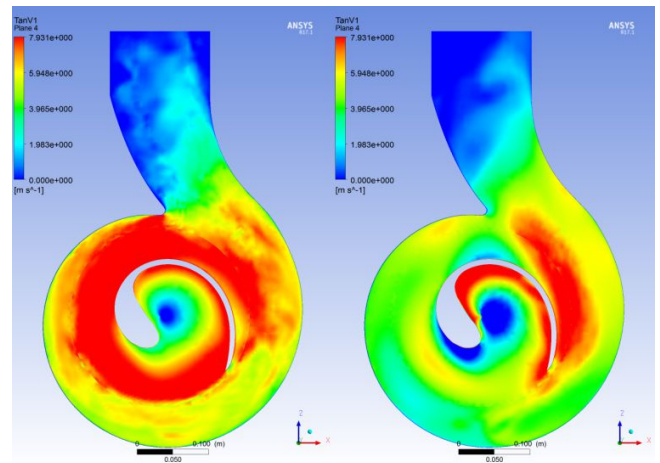


Figure 8 Tangential Velocity on Plane 4 at $Q^*=0.68$ (left) and $Q^*=1.11$ (right)

Figure 8 shows a much higher incidence of tangential velocity at low flow rate compared to high flow rate. Given that as the fluid is more inclined to recirculate the rag has a higher probability of impacting the leading edge and blocking the impeller. The low level of tangential velocity existing at the leading edge at $Q^*=1.11$ where high radial velocity is present in Figure 6-3, makes it possible to infer that the flow is almost purely radial.

What is notable, especially in the high flow condition, is the occurrence of two areas of high tangential velocity [Figure 8]. The region of high v_{tan} on the suction surface of the impeller is caused by the flow following the curvature of the impeller and the flow incident angle. The other area of high tangential velocity is caused by the impeller accelerating the fluid, due to centrifugal force, tangentially towards the volute outlet. Studying other positions of the impeller relative to the volute shows similar occurrences [Figure 9].

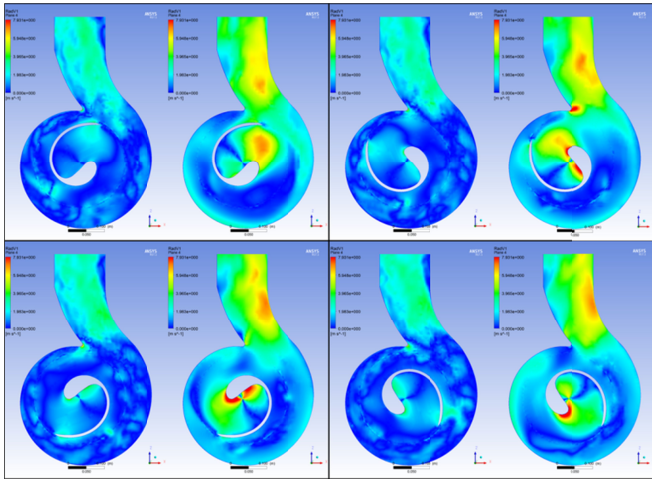


Figure 9 Radial Velocity at $Q^*=0.68$ (left) and $Q^*=1.11$ (right) for each of the four impeller positions studied.

Comparing the radial velocity at different impeller positions between the two pump flow rates clearly confirms its increase in proportion to the flow rate [Figure 9]. This should contribute to the rag being more quickly ejected away from the leading edge at high flow rates. This is confirmed by experimental observations made with the high speed camera which clearly show that rather than being caught either side of the leading edge and blocking, the rag when subjected to higher radial velocity components has now been moved clear of the leading edge. It is important to also consider the inlet flow field, as it is a factor in how the rag is presented to the pump impeller. Higher radial velocity can be observed at analysis plane 2, at the pump inlet at high flow rate, when compared to low flow rate [Figure 10]. It can be argued that regardless of the rag position or orientation when entering the pump, a strong radial flow will help to move it outwards past the impeller leading edge once it has passed through the inlet.

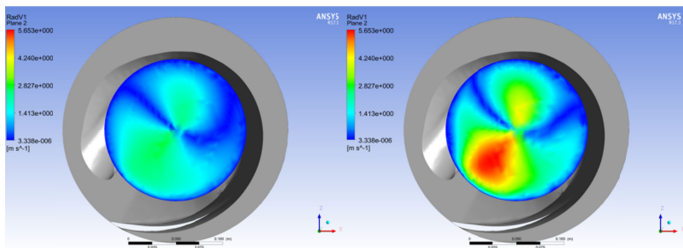


Figure 10 v_{rad} at pump inlet plane at $Q^*=0.68$ (left) and $Q^*=1.11$ (right)

Considering both contour plots and iso-surfaces helps inform the overall behaviour of the flow. A comparison of velocity components in the domain provides a better quantitative description of how these components vary with flow rate, most importantly at the impeller leading edge, the area of the pump with the highest probability of blocking. To further investigate the relationship between v_{rad} and v_{tan} at high and low flow rates, a rake line was imposed onto analysis plane 4, 11mm in advance of the impeller leading edge, as shown in [Figure 6-10].

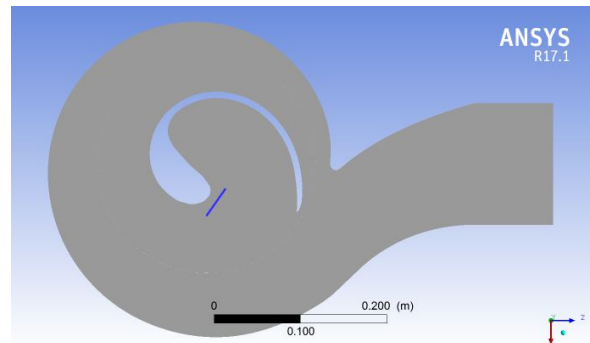


Figure 11 Rake line on plane 4 at impeller position 1
A rotation matrix was used to perform a rotational transformation on the rake line in order to consistently study comparable velocity profiles at each of the 4 impeller positions.

Plotting the profiles of v_{rad} and v_{tan} at each impeller position shows the difference between each velocity type at low and high flow rates at impeller position 1, [Figure 12]. It is clear that v_{rad} is the largest velocity component at high flow rate by as much as a factor of 2. Conversely, at low flow rate v_{tan} is the dominant component with a magnitude 3 to 5 times higher than v_{rad} . Also notable is when the same comparison is made at impeller position 4 [Figure 13] the difference between both components is higher at both flow rates. This indicates that blockage may be more likely to occur at impeller position 1 than at impeller position 4. The instantaneous rotational velocity of the leading edge, v_{rot} , at each position is an important consideration as it can be compared to v_{rad} and v_{tan} to assess how quickly the impeller can catch up with the rag before it can be ejected into the volute.

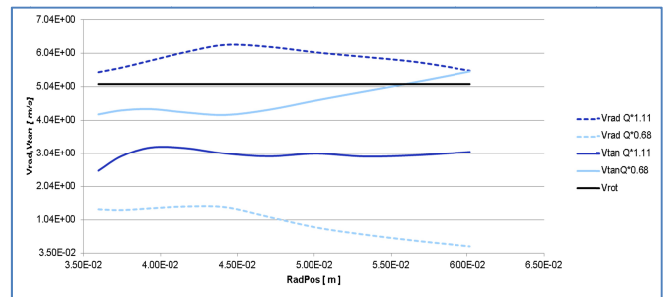


Figure 12 v_{rad} , v_{tan} on Impeller Rake Line and Leading Edge Rotational Speed, v_{rot} at Impeller Position 1

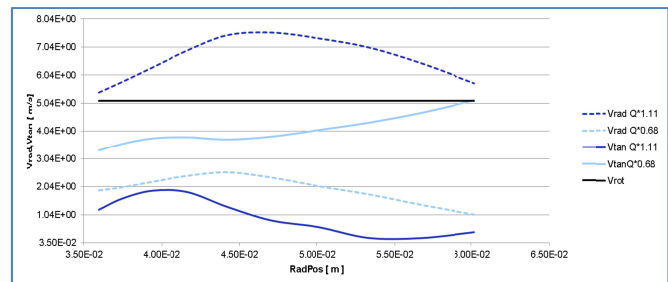


Figure 13 v_{rad} , v_{tan} on Impeller Rake Line and Leading Edge Rotational Speed, v_{rot} at Impeller Position 4

It can be suggested that as v_{rad} is the largest velocity component at high flow rates including when compared to the impeller rotational speed, the rag can move out of the way more quickly than the impeller can catch it [Figure 12 and Figure 13]. Also if v_{tan} is greater than v_{rot} then the impeller should never catch up with the rag. As this has not been observed over the entire course of testing it can be concluded that v_{tan} is not significant a factor for blockage performance as v_{rad} .

CONCLUSION

In this study a comparison of experimental and computational analyses has shown that most pumps perform better at resisting soft blockage at high flow rates compared to low flow rates. A new test rig was designed and a new test material was chosen in order to compare pumps of different sizes and at different design points. An analysis of factors which may contribute to blockage resulted in a dimensionless number which could in future be used to describe how probable the occurrence of pump blockage is with a view to informing future designs. Based on these results an observational analysis was performed with high speed photography at each flow rate with all test pumps to inform on the possible causes of soft blockages. The CFD analysis was performed to attempt to describe the processes responsible for leading edge blockage, the most common type of blockage observed. The study focussed on a comparison of radial and tangential flow components over 5 planes along the axis of the impeller. Results suggested that the higher radial velocity obtained at higher pump flow rates helps flush the rag as it flows from the inlet sum through the impeller radially, away from the leading edge before contact can occur. The higher tangential component observed at low flow rates also compound the risk of blockage by increasing the likelihood of the flow to carry the rag towards the leading edge. It was also suggested that impeller position in the volute can have an effect on blockage performance. This may not be significant in physical testing, as the average inlet velocity at $Q^*=1.11$ is $3.87m/s$, compared with a leading edge velocity of $4.7m/s$. By the time the rag has travel 40 mm through the inlet of the pump the impeller has already rotated by 90.4° .

REFERENCES

- [1] JMP, "WHO/UNICEF Joint Monitoring Programme for Water Supply and Sanitation," October 2016. [Online]. Available: <http://www.wssinfo.org/definitions-methods/>. [Accessed October 2016].
- [2] H. e. a. Korving, "Statistical Modelling of the Serviceability of Sewage Pumps," *Journal of Hydraulic Engineering*, vol. 132, no. 10, pp. 1076-1085, 2006.
- [3] Health Research Inc, "Policies for the Design, Review, and Approval of Plans and Specifications for Wastewater Collection and Treatment Facilities," Albany, NY, 2004.
- [4] R. McEvoy, "Innovative Development of Single-Blade-Impeller Hydraulics for Wastewater Application," Limerick, 2011.
- [5] R.-L. Mitchell, Investigations into wastewater composition focusing on nonwoven wet wipes, Berlin: Technical Transactions, 2017.
- [6] T. S. Kevin A Kaupert, "The Unsteady Pressure Field in a High Specific Speed Centrifugal Pump Impeller," *Journal of Fluids Engineering*, pp. 621-632, 1999.
- [7] A. N. R. M. B. de Souza, "A numerical investigation of the Consant Velocity Volute Design Approach as Applied to the Single Blade Impeller," *Journal of Fluids Engineering*, p. vol. 132, 2010.
- [8] Y. Delauré, "CFD Modelling of Turbulent Incompressible Flow for Pumping/Mixing Applications," Dublin, 2016.
- [9] R. Nichols, "Turbulence Models and Their Application to Complex Flows," University of Alabama, Birmingham, Rev 4.01.
- [10] O. M. Paresh Girdhar, Practical Centrifugal Pumps, Elsevier, 2011.
- [11] F.-K. B. H. D. J. Feng, "Unsteady Flow Visualisation at Part-Load Conditions of a Radial Diffuser Pump: by PIV and CFD," *Journal of Visualization*, pp. 65-72, 2009.
- [12] C. B. J. N. P. Rikke K. Byskov, "Flow in a Centrifugal pump Impeller at Design and Off-Design Conditions - PartII: Large Eddy Simulations," vol. 125, 2003.
- [13] J. F. Gülich, Centrifugal Pumps, Heidelberg: 2008, 2008.